EAST EUROPEAN JOURNAL OF PHYSICS. **1.** 96-104 (2022)
DOI:10.26565/2312-4334-2022-1-13 ISSN 2312-4334

FLUORESCENCE STUDY OF THE INTERACTIONS BETWEEN INSULIN AMYLOID FIBRILS AND PROTEINS†

Uliana Tarabara*, Olga Zhytniakivska, Kateryna Vus, Valeriya Trusova, Galyna Gorbenko
Department of Medical Physics and Biomedical Nanotechnologies, V.N. Karazin Kharkiv National University
4 Svobody Sq., Kharkiv, 61022, Ukraine
**Corresponding Author: uliana.tarabara@karazin.ua*
Received January 15, 2022, revised January 22, 2022; accepted January 23, 2022

Self-assembly of proteins and peptides into amyloid fibrils is the subject of intense research due to association of this process with multiple human disorders. Despite considerable progress in understanding the nature of amyloid cytotoxicity, the role of cellular components, in particular proteins, in the cytotoxic action of amyloid aggregates is still poorly investigated. The present study was focused on exploring the fibril-protein interactions between the insulin amyloid fibrils and several proteins differing in their structure and physicochemical properties. To this end, the fluorescence spectral properties of the amyloid-sensitive fluorescent phosphonium dye TDV have been measured in the insulin fibrils (InsF) and their mixtures with serum albumin (SA) in its native solution state, lysozyme (Lz) and insulin (Ins) partially unfolded at low pH. It was found that the binding of TDV to the insulin amyloid fibrils is followed by considerable increase of the fluorescence intensity. In the system (InsF + TDV) the TDV fluorescence spectra were decomposed into three spectral components centered at ~ 572 nm, 608 nm and 649 nm. The addition of SA, Lz or Ins to the mixture (InsF + TDV) resulted in the changes of the fluorescence intensity, the maximum position and relative contributions ($f_{1,3}$) of the first and third spectral components into the overall spectra. The Förster resonance energy transfer between the TDV as a donor and a squaraine dye SQ1 as an acceptor was used to gain further insights into the interaction between the insulin amyloid fibrils and proteins. It was found that the presence of SA do not change the FRET efficiency compared with control system (InsF + chromophores), while the addition of Lz and Ins resulted in the FRET efficiency decrease. The changes in the TDV fluorescence response in the protein-fibril systems were attributed to the probe redistribution between the binding sites located at InsF, the non-fibrillized Ins, SA or Lz and protein-protein interface
Keywords: phosphonium probe, insulin amyloid fibrils, fibril-protein complexation.
PACS: 87.14.C++c, 87.16.Dg

A conformational space of protein molecules includes a variety of structures differing in their free energy, among which are unfolded, partially folded and native structural states, oligomers, amorphous aggregates and amyloid fibrils [1-4]. Of these, most attention has been paid in the last decade to the amyloid fibril state of a polypeptide chain [1-4]. A distinctive feature of this state is the presence of cross-β core in which intermolecular b-sheets propagate along the main fibril axis [5], resulting in a characteristic X-ray diffraction picture with reflections corresponding to separation of b-sheet strands (~0.5 nm) and spacing between b-sheet layers (1 nm), respectively [6]. Amyloid fibrils are currently a subject of keen interest, mostly in biomedical and nanotechnological aspects [7,8]. Multiple lines of evidence indicate that fibrillar protein aggregates and their precursors are involved in the development of more than forty human disorders, such as neurological diseases, systemic amyloidosis, type II diabetes, etc. [9,10]. The amyloid assemblies have been found both in intracellular and extracellular space and their cytotoxicity is primarily associated with the impairment of cell membranes [11,12]. The structurally flexible early oligomeric intermediates with extensive hydrophobic areas have been shown to cause membrane disintegration [13,14], formation of non-specific ionic channels [15], uptake of membrane lipids [16,17], etc. Furthermore, it has been demonstrated that not only protein oligomers, but an ensemble of cross-b-sheet-rich protein aggregates including mature fibrils display a high cytotoxic potential. Specifically, mature lysozyme fibrils have been reported to produce hemolysis of erythrocytes [14], mitochondrial failure and increase of plasma membrane permeability [18]. However, it seems likely that membranes are not the only target for cytotoxic action of amyloid aggregates and other cellular components, such as proteins can be affected by amyloids under in vivo conditions. In view of this, the aim of the present study was to explore the interactions between the insulin amyloid fibrils and several proteins differing in their structure and physicochemical properties, viz. serum albumin (SA) in its native solution state, lysozyme (Lz) and insulin (Ins) partially unfolded at low pH. The amyloid-sensitive fluorescent phosphonium dye TDV was employed to monitor the fibril-protein complexation.

EXPERIMENTAL SECTION

Materials

Bovine insulin (Ins), bovine serum albumin (BSA), egg yolk lysozyme (Lz), Tris and thioflavin T (ThT) were purchased from Sigma. The phosphonium dye TDV and squaraine dye SQ1 were kindly provided by Prof. Todor

† ***Cite as***: U. Tarabara, O. Zhytniakivska, K. Vus, V. Trusova, and G. Gorbenko, East. Eur. J. Phys. **1**, 96 (2022), https://doi.org/10.26565/2312-4334-2022-1-13

Deligeorgiev (Faculty of Chemistry, University of Sofia, Bulgaria). All other reagents were of analytical grade and used without the further purification. The structural formulas of the employed fluorescent dyes are shown in Fig. 1.

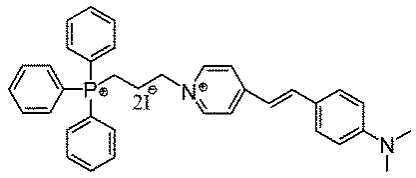

TDV

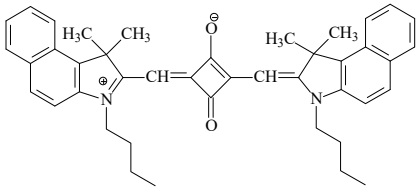

SQ1

Figure 1. Chemical structures of the employed fluorophores.

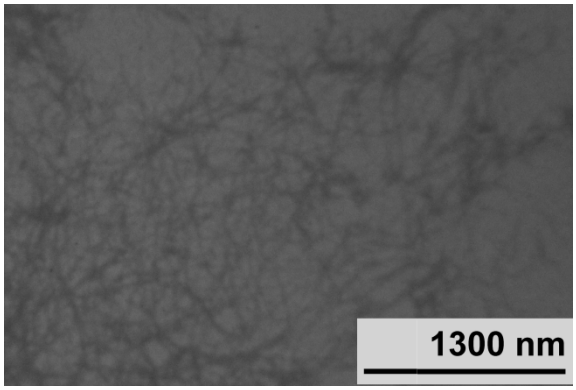

Figure 2. Transmission electron microscopy photograph of insulin amyloid fibrils.

Preparation of working solutions

The insulin solution (10 mg/ml) was prepared by dissolving the protein in 10 mM glycine buffer (pH 2.0). To prepare the amyloid fibrils, this solution was subjected to constant agitation on the orbital shaker at 37 °C. The stock solutions of ThT and TDV were prepared in 10 mM Tris-HCl buffer (pH 7.4), while SQ1 was dissolved in dimethyl sulfoxide. The concentrations of the protein and dyes were determined spectrophotometrically using the extinction coefficients $\varepsilon_{277} = 6.1 \cdot 10^3$ $M^{-1}cm^{-1}$ (Tyr residues of insulin, [19]), $\varepsilon_{412} = 3.6 \cdot 10^4$ $M^{-1}cm^{-1}$ (ThT, [20]), $\varepsilon_{676} = 2.3 \cdot 10^5$ $M^{-1}cm^{-1}$ (SQ1, [21]), $\varepsilon_{480} = 2.05 \cdot 10^4$ $M^{-1}cm^{-1}$ (TDV). The amyloid nature of the protein aggregates was confirmed by ThT assay and the transmission electron microscopy (Fig. 2). To monitor the kinetics of ThT fluorescence, the aliquots of insulin solution (10 µl) were withdrawn every 24 hours and added to ThT solution in Tris-HCl buffer (3.72 µM), with subsequent recording of the dye fluorescence spectra.

TEM measurements

The samples for the transmission electron microscopy assay were prepared as follows: a 10 µl drop of the insulin solution (378 µM) in Tris-HCl buffer (pH 7.4) was applied to a carbon-coated grid and blotted after 1 min. A 10 µl drop of 1.5% (w/v) phosphotungstic acid solution was placed on the grid, blotted after 30 s, and then washed 3 times by deionized water, air dried and viewed at 75 kV by a Selmi EM-125 electron microscope (Selmi, Ukraine).

Fluorescence measurements

The fluorescence measurements were carried out in 10 mM Tris-HCl buffer (pH 7.4) with a Perkin-Elmer FL-6500 spectrofluorometer (Perkin Elmer, UK). The steady-state fluorescence spectra of TDV were recorded at 25 °C within the range of 490–750 nm at the excitation wavelength of 470 nm using 10 mm path length quartz cuvettes. The excitation and emission slit widths were set at 10 nm.

Deconvolution of fluorescence spectra and FRET data analysis

The deconvolution of the total fluorescence spectra of TDV into separate peaks was performed with the Origin software (version 9.4) using the log-normal asymmetric function [22]:

$$I = I_{\max} \exp\left[-\frac{\ln 2}{\ln^2(\rho)} \ln^2\left(\frac{a-\nu}{a-\nu_c}\right)\right] \tag{1}$$

where ν is the wavenumber, I is the fluorescence intensity on the wavenumber scale $I(\nu) = \lambda^2 I(\lambda)$ [23]; $I_{\max} = I(\nu_c)$ is the fluorescence intensity maximum (the peak amplitude), ν_c is the peak center; $\rho = (\nu_c - \nu_{\min})/(\nu_{\max} - \nu_c)$ is the asymmetry of the band, $\nu_{\max}$ and $\nu_{\min}$ are the maximum and minimum wavenumber values at the half-amplitude; $a = \nu_c + (\nu_{\max} - \nu_{\min}) \cdot \rho / (\rho^2 - 1)$ is the limiting wavenumber, after reaching which the peak intensity becomes equal to zero.

The FRET efficiencies were determined from the decrease of the TDV fluorescence in the presence of SQ1 [23]:

$$E = 1 - \frac{I_{DA} k}{I_D} \tag{2}$$

where I_D, I_{DA} are the donor fluorescence intensities in the absence and presence of the acceptor, respectively; $k = 10^{(A_a^{ex} + A_a^{em})/2}$ is the inner filter effect correction factor; A_a^{ex} and A_a^{em} are the acceptor absorbance at the donor excitation and emission wavelengths, respectively. The Förster radii were calculated for each donor-acceptor pair using the Mathcad 15.0 software (PTC) as [23]:

$$R_0 = 979\left(\kappa^2 n_r^{-4} Q_D J\right)^{1/6},\ J = \int_0^\infty F_D(\lambda)\varepsilon_A(\lambda)\lambda^4 d\lambda \Big/ \int_0^\infty F_D(\lambda) d\lambda \tag{3}$$

where J is the overlap integral derived from numerical integration; $F_D(\lambda)$ is the donor fluorescence intensity; $\varepsilon_A(\lambda)$ is the acceptor molar absorbance at the wavelength λ; n_r is the refractive index of the medium; Q_D is the donor quantum yield; κ^2 is the orientation factor, depending on the relative spatial orientation of the donor and acceptor transition dipoles. The quantum yield of the donor required for the calculation of the Förster radius, was estimated as:

$$Q_D = \frac{Q_{st}\left(1 - 10^{-A_{st}}\right) S_D}{\left(1 - 10^{-A_D}\right) S_{st}} \frac{n_D^2}{n_{st}^2} \tag{4}$$

where subscripts *D* ans *st* refer to the donor dye and standard, respectively; A_D, A_{st} are the optical densities at the excitation wavelength; S_D, S_{st} are the integrated areas of fluorescence spectra; n_D, n_{st} are the refractive indexes of the dye solutions. The standard used for TDV was Rhodamine 6G in water (Q_{st} =0.93). In the fibril-bound state the quantum yield of TDV was found to be 0.11. To obtain the quantitative estimates for the average donor-acceptor separation, the results of FRET measurements were treated in terms of the classical expression for the distance dependence of FRET efficiency:

$$E = \frac{R_0^6}{R_0^6 + R^6};\qquad R = R_0\left(1/E - 1\right)^{1/6} \tag{5}$$

RESULTS AND DISCUSSION

As illustrated in Fig. 3A, the binding of TDV to the insulin amyloid fibrils (InsF) is followed by considerable increase of the fluorescence intensity (more than 30-fold at the emission maximum 610 nm), arising presumably from the reduced polarity and mobility of the dye molecular environment. Using the previously determined quantitative parameters of the TDV-InsF complexation (the association constant - $28.6^{\pm 5.4}$ μM^{-1}, the binding stoichiometry - $0.07^{\pm 0.013}$ [24]), the fraction of the fibril-bound under the employed experimental conditions dye was estimated to be ~ 26% (0.23 μM at InsF and TDV total concentrations 3.5 μM and 0.9 μM, respectively). Furthermore, it appeared that the TDV fluorescence spectra can be decomposed into three spectral components centered for the system (InsF + TDV) at ~ 572 nm, 608 nm and 649 nm (Table 1).

Table 1. Spectral characteristics of TDV in the presence of insulin fibrils and proteins

System	Band	A_{max}*	λ_c, nm	FWHM, nm	f, %	R^2
TDV in free state	I	768.9	578.2	78.5	27	0.998
	II	1740.2	622	68.4	45	
	III	286.1	655.8	169.7	28	
TDV+InsF	I	19885.9	572	53.6	17.9	0.998
	II	80601.0	608.8	50	51.5	
	III	37796.3	649.2	57.25	30.6	
(TDV+InsF)+BSA	I	30803.0	578.9	63.4	34.8	0.998
	II	51435.6	613.8	58.8	51.6	
	III	9602.0	670	69.9	13.6	
(TDV+InsF)+Lz	I	28105.8	579.9	74.9	64.5	0.997
	II	15283.5	608.9	49.5	23.9	
	III	4380.0	647.6	62.9	11.6	
(TDV+InsF)+Ins	I	99120.9	587.1	83.5	71.4	0.998
	II	53455.5	605.7	43.6	20.5	
	III	11579.5	648.8	61.8	8.1	

*the maximum fluorescence intensity is given after baseline subtraction

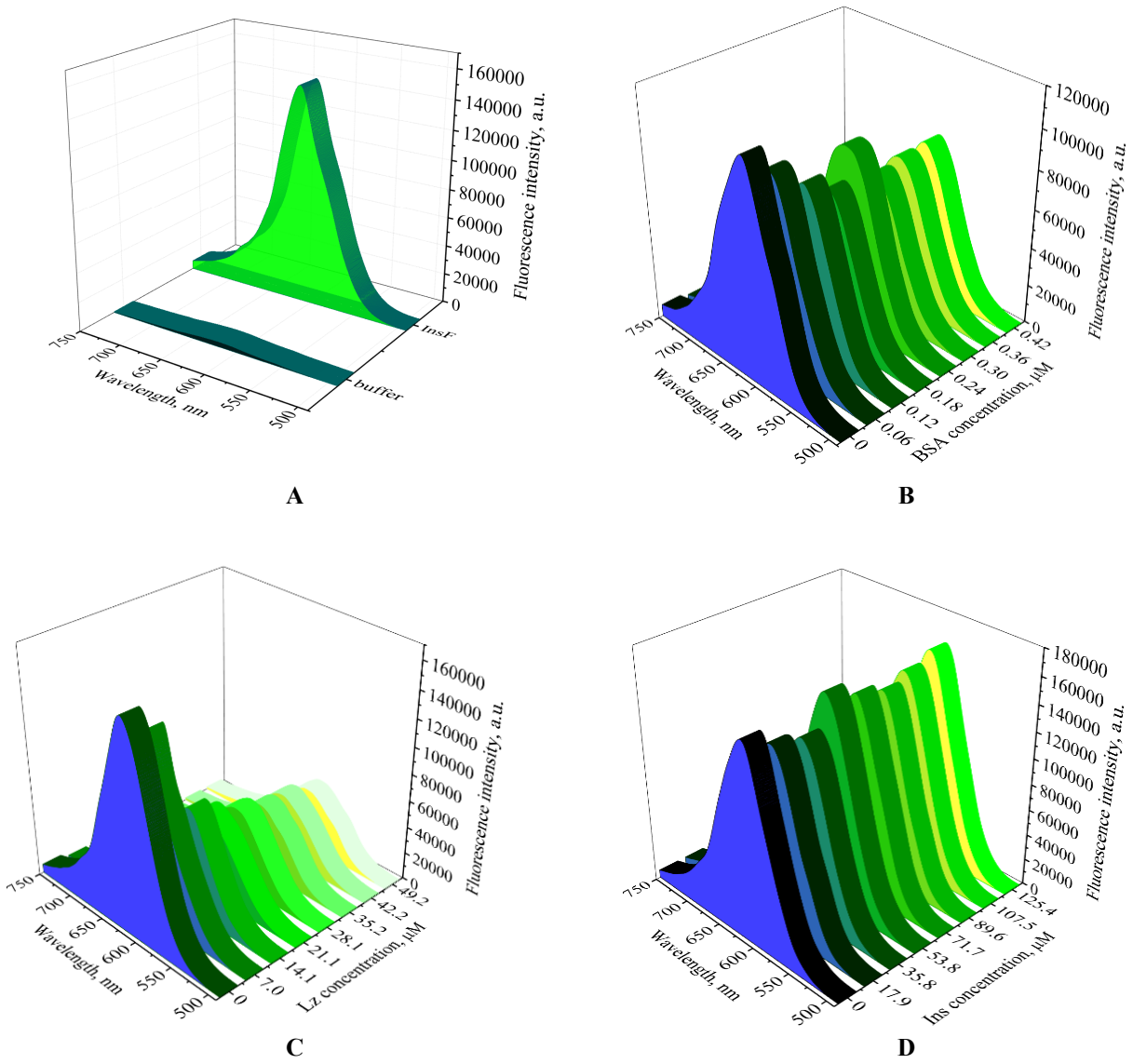

Figure 3. TDV fluorescence spectra in buffer and in the presence of insulin fibrils (**A**). The fluorescence spectra of TDV in the fibril-bound state at the increasing concentration of serum albumin (**B**), lysozyme (**C**) and insulin (**D**). InsF concentration was 3.5 μM, dye concentration was 0.9 μM.

Three bands in the dye fluorescence spectra in the system (InsF + TDV) most probably result from the existence of the different modes of TDV binding to the insulin fibrils. In our previous studies we demonstrated that the solvent-exposed groove Gln15_Glu17 provides the most energetically favorable binding sites for TDV due to electrostatic interactions between a negatively charged side chain of glutamic acid and TDV molecule which bears two positive charges localized on phosphorus and nitrogen atoms [24]. Moreover, it was shown that TDV only partially inserts into Gln15_Glu17 groove, adopting a non-planar conformation. However, due to the preference of TDV and classical amyloid marker ThT to the same binding sites [24], we cannot rule out the possibility of TDV accumulation in the clustered areas of fibril network (the cavities formed between the intertwined insulin fibrils) as was previously demonstrated for ThT [25].

Next, the amyloid-sensitive fluorescent phosphonium dye TDV was employed to monitor the interactions between the insulin amyloid fibrils and proteins such as serum albumin, lysozyme or insulin in the non-fibrillized form (Fig 3, Fig 4). The addition of BSA to the mixture (InsF + TDV) resulted in the decrease of fluorescence intensity coupled with the changes in the maximum position and relative contributions ($f_{1,3}$) of the first and third spectral components into the overall spectra (Fig. 3B, Fig. 4A). As seen in Table 1, BSA gives rise to f_1 increase (from 18% to 35%) and f_3 decrease (from 31% to 14%), along with the red shift of the position of band I, band II and band III for 6.9 nm, 5 nm and 20.8 nm, respectively, compared with the system (TDV+InsF). These effects were accompanied by the broadening of all

bands relative to the TDV spectral components in InsF. Only limited information is available up to now about interaction between albumins and mature amyloid fibrils. In particular, albumin has been reported to inhibit the amyloid-β fibrillization through affecting the conformational ensemble of Aβ by nonspecific interactions only at the initial stage of the Aβ aggregation [26]. Likewise, Siposova et al. have demonstrated that albumin-modified magnetic fluids are able to destroy the insulin amyloid fibrils in vitro [27]. To ascertain whether the observed spectral changes are the result of direct TDV-BSA interaction or due to the TDV sensitivity to the BSA-induced changes in the insulin amyloid fibrils, we measured the fluorescence spectra of TDV in the presence of BSA (without InsF). It appeared that TDV-BSA complexation leads to the fluorescence intensity increase only up to 2.3 times (data not shown) with 15-nm hypsochromic shift.

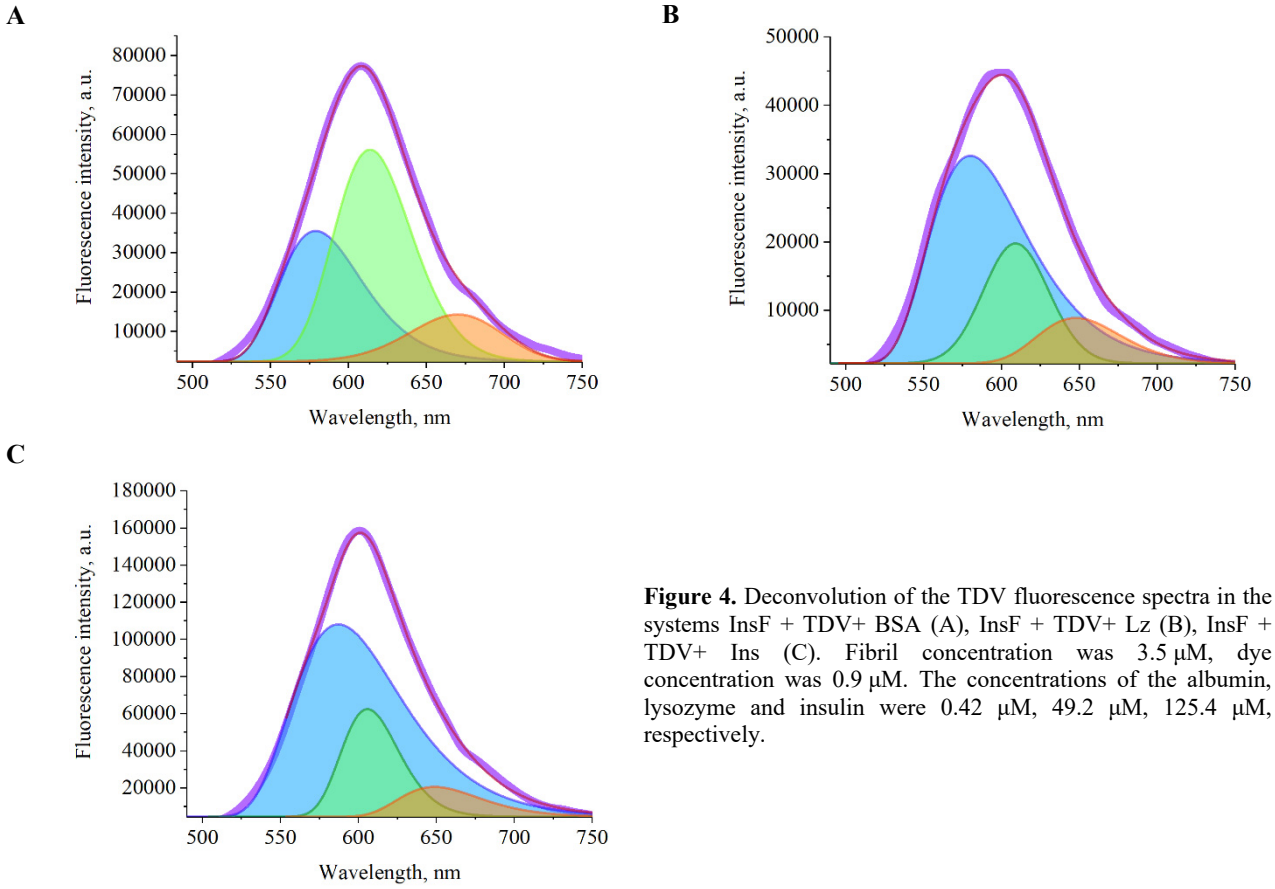

Figure 4. Deconvolution of the TDV fluorescence spectra in the systems InsF + TDV+ BSA (A), InsF + TDV+ Lz (B), InsF + TDV+ Ins (C). Fibril concentration was 3.5 μM, dye concentration was 0.9 μM. The concentrations of the albumin, lysozyme and insulin were 0.42 μM, 49.2 μM, 125.4 μM, respectively.

Therefore, the aforementioned spectral changes most likely reflect the redistribution of TDV molecules between the binding sites located at InsF, BSA and protein-protein interface. Given that at pH 7.4 BSA bears a negative charge [28], the redistribution of the positively charged TDV in the presence of BSA is most probably driven by the electrostatic attraction between BSA and TDV. Numerous studies indicate that the principal ligand-binding sites are located in hydrophobic cavities in bovine serum albumin subdomains, referred to as site I and site II according to terminology proposed by Sudlow et al [29]. Moreover, the positively charged dyes (cyanines, squaraines, etc.) generally exhibit a higher specificity to the binding site II of albumins [30,31], so it can be hypothesized that the same mode of binding is realized in our system.

Interestingly, while comparing the fluorescence spectra of TDV+InsF in the presence of the positively charged lysozyme and negatively charged albumin, it becomes evident that the spectral changes induced by Lz are more drastic than those observed for BSA (Fig. 3C, Fig. 4B). More specifically, the addition of lysozyme to the TDV+InsF system resulted in 1.4-fold enhancement of the fluorescence intensity of band I along with a marked drop in the amplitude of the band II (5.3 times) and band III (8.6 times). This effect was accompanied with ~ 8 nm bathochromic shift of the position of band I coupled with the broadening of bands I and III (Table 1). Moreover, the addition of Lz to the mixture (InsF + TDV) produced the changes in the relative contributions ($f_{1,3}$) of the first and third spectral components into the overall spectra, more significant in comparison with those observed in the presence of BSA (Fig. 3B, Fig. 4A). As seen in Table 1, Lz gives rise to f_1 increase (from 18% to 65%) and f_3 decrease (from 31% to 12%).

More pronounced fluorescence decrease and the changes of spectral profile in the presence of the positively charged Lz (Fig. 5B, Fig. 6B), is indicative of essential contribution of electrostatic interactions to stabilization of the protein-fibril and dye-protein complexes. Notably, in the absence of insulin fibrils Lz insignificantly influenced the TDV spectral response, giving rise to only 1.2-fold enhancement of the dye fluorescence. One of the most probable

reason for the drastic decrease of TDV fluorescence after lysozyme addition to the TDV+InsF mixture seems to lie in the competition between the positively charged probe and lysozyme for the binding sites on the insulin amyloid fibrils. It is well known that electrostatic interactions play a crucial role in the complexation of lysozyme with lipid membranes [32, 33], nanoparticles [34] and drugs [35]. Therefore, it is highly probable that electrostatic interactions of the positively charged lysozyme with the solvent-exposed negatively charged amino acid residues of InsF partially block TDV binding sites on the insulin fibrils, thereby causing the TDV fluorescence decrease.

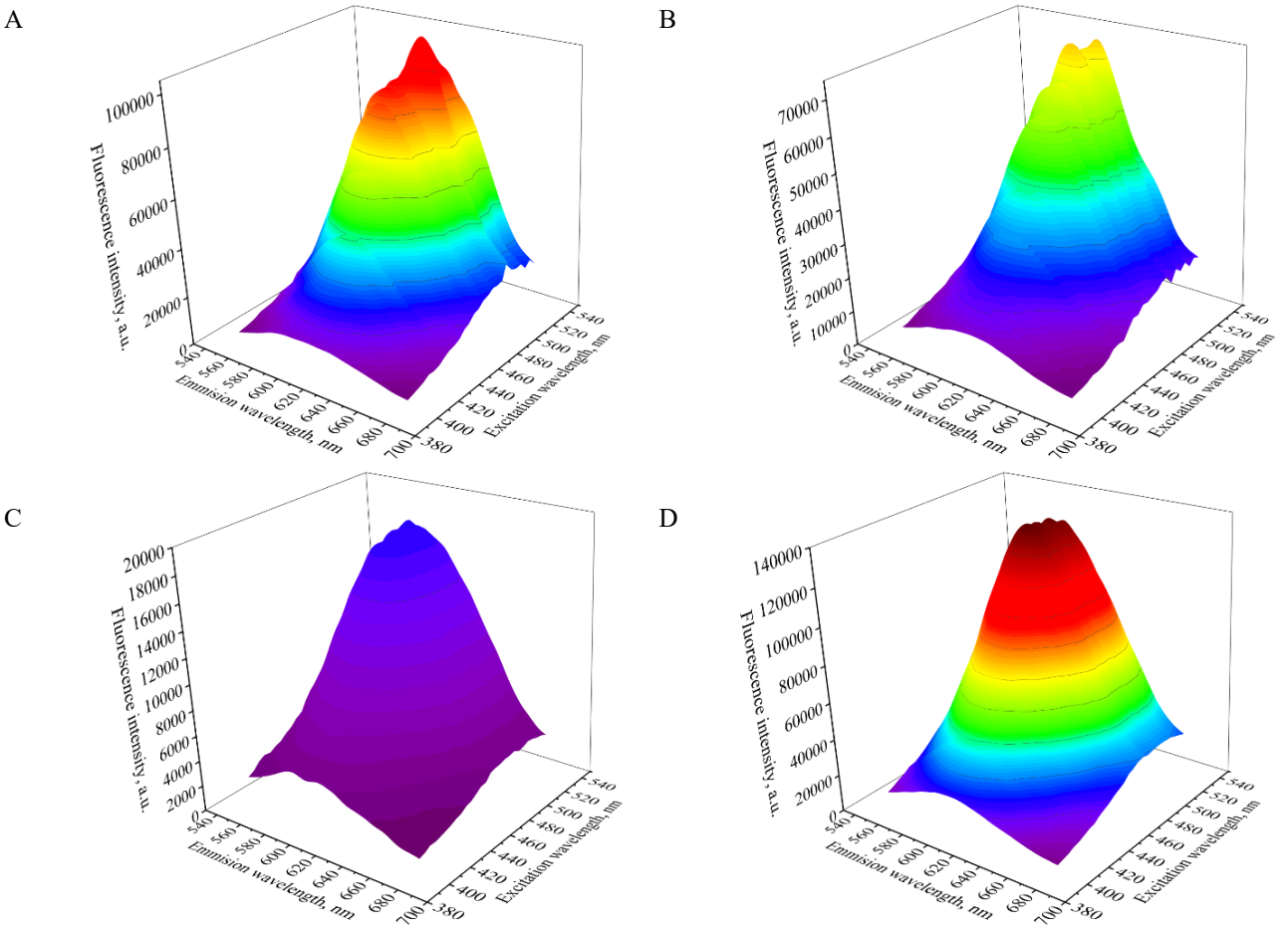

Figure 5. 3D fluorescence spectra of the systems TDV+InsF (A) and after BSA (B), Lz (C) and Ins (D) addition. The emission and excitation wavelengths were varied within the ranges 580-680 nm and 400-530 nm, respectively. The excitation and emission slit widths were set at 10 nm. The false color scale ranging from 1050 a.u. (violet) to 136500 a.u. (red) was used for fluorescence intensity.

The addition of partially unfolded insulin to the system (TDV+InsF) resulted in a slight fluorescence intensity increase coupled with the alterations in the maximum position and relative contributions ($f_{1,3}$) of the first and third spectral components into the overall spectra (Fig. 3D, Fig. 4C). More specifically, the addition of partially unfolded insulin to the system (TDV+InsF) the following spectral changes were observed:

1) increase of the band I intensity (5 times), coupled with a slight attenuation of the band II (1.5 times) and band III (3.3 times);
2) rise of the relative contribution of the first spectral component f_1 (from 18% to 71%) and decrease in that of the third component f_3 (from 31% to 8%);
3) broadening of all spectral bands.

The above spectral changes most likely reflect the redistribution of TDV molecules between the binding sites located at InsF, the partially unfolded insulin and protein-protein interface. The comparison of the spectral responses of TDV in the presence of negatively charged proteins serum albumin and insulin shows that the spectral changes induced by Ins are more drastic. One of the most probable reason for the above effect is a strong affinity of TDV for the insulin partially unfolded at low pH. We observed that the TDV binding to Ins leads to the 17-fold fluorescence increase along with a 21-nm hypsochromic shift of the emission maximum (data not shown). It seems that the electrostatic interactions TDV and Ins/BSA play the predominant role in the TDV-protein complexation and strong hydrophobicity of the BSA binding sites hampers the dye association with this protein. This finding is also

confirmed by the distinct 3D fluorescence patterns of TDV in the examined systems. As seen in Fig. 5, in the presence of the partially unfolded Ins TDV displays a more-intensive 3D pattern than that in the TDV+InsF system. Likewise, the addition of BSA and Lz led to the decrease in the intensity of 3D fluorescence spectra, being more pronounced for lysozyme.

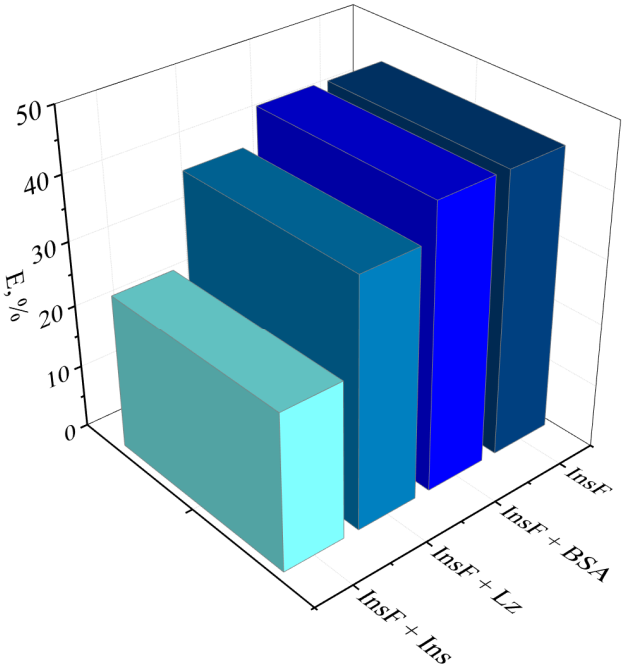

Figure 6. Efficiencies of energy transfer for the donor-acceptor pair TDV-SQ1 in different systems.

At the next step of the study the Förster resonance energy transfer between TDV as a donor and a squaraine dye SQ1 as an acceptor was used to study the interaction between the insulin amyloid fibrils and serum albumin, lysozyme and insulin. Our previous findings indicate that insulin amyloid fibrils can serve as a scaffold for TDV and SQ1, so the energy can be transferred between these fluorophores by a distance-dependent Förster mechanism [24]. The addition of SQ1 to the TDV+InsF system in the absence and presence of the non-fibrillized proteins led to significant quenching of the TDV fluorescence with the magnitude of this effect being dependent on the protein. Using the previously determined FRET parameters for the donor-acceptor pair TDV-SQ1, *viz.* the Förster radius (4.75 nm) and overlap integral (6.68×10^{15} $M^{-1}cm^{-1}nm^4$) [24], the efficiencies of energy transfer in different systems were estimated from the decrease of TDV fluorescence (at 600 nm) in the presence of SQ1 (Fig. 6). It appeared that BSA does not affect the FRET efficiency compared with control system (InsF + chromophores), while the addition of Lz and Ins resulted in the decrease of this paramer (by 5.3 % and 19.5 %, respectively). The average interchromophore distances for the donor-acceptor pair TDV-SQ1 were estimated to fall in the range from 4.9 nm (for InsF and InsF+BSA systems) to 5.7 nm (for InsF+Ins system).

Presented in Fig.7 are 3D fluorescence spectra of the donor-acceptor pair TDV-SQ1 recorded in the presence of InsF, (InsF + BSA), (InsF + Lz) and (InsF + Ins) at the emission and excitation wavelengths covering the range 550-750 nm and 400-452 nm, respectively. More specifically, in the presence of the insulin fibrils the 3D pattern is highly-intensive with the two well-defined and comparable by the intensity maxima centered at ~ 620 nm and ~680 nm, corresponding to emission of fibril-bound TDV and SQ1, respectively. The addition of albumin or lysozyme to the system (InsF + chromophores) gives rise to the decrease of the fluorescence signal for both TDV and SQ1 dyes. Notably, the system (InsF + chromophores + Ins) displays highly emissive 3D pattern where the TDV fluorescence signal is significantly greater than that of SQ1. Obviously, the redistribution of TDV and SQ1 driven by their strong affinity to the partially unfolded at low pH insulin resulted in the decreased amount of the acceptor SQ1 in the proximity to the donor (required for the effective FRET) leading to the decrease of the energy transfer rate in the system InsF + Ins.

CONCLUSIONS

In summary, the present study demonstrated that the amyloid-sensitive fluorescent phosphonium dye TDV can be employed for the characterization of the interactions between the insulin amyloid fibrils and several proteins differing in their structure and physicochemical properties. Based on the comprehensive analysis of the spectral characteristics of TDV in the amyloid fibrils and in the presence of serum albumin (in its native solution state), lysozyme or insulin (partially unfolded at low pH) we observed the changes of the fluorescence intensity, the maximum position and relative contributions of the first and third spectral components into the overall spectra after the protein addition to the mixture (InsF + TDV). These effects presumably reflect the redistribution of TDV

molecules between the binding sites located at InsF, the non-fibrillized Ins, BSA or Lz and protein-protein interface.

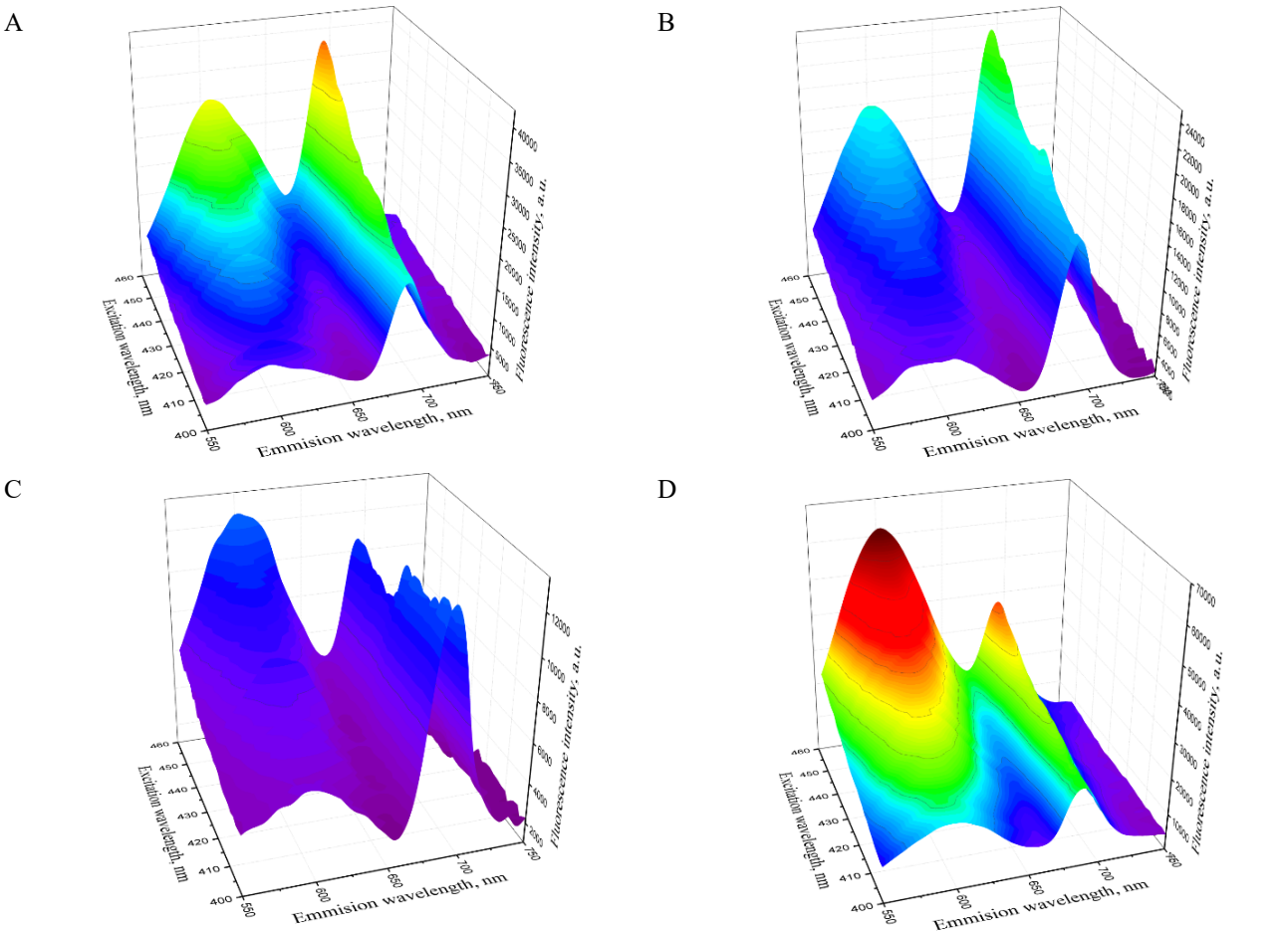

Figure 7. 3D fluorescence spectra of the donor-acceptor pair TDV-SQ1 recorded in the presence of InsF (A), InsF + BSA (B), InsF + Lz (C) and InsF + Ins (D). The emission and excitation wavelengths were varied within the ranges 550-750 nm and 400-452 nm, respectively. The excitation and emission slit widths were set at 10 nm. The false color scale ranging from 800 a.u. (violet) to 65800 a.u. (red) was used for fluorescence intensity. SQ1 concentration was 0.35 μM.

ACKNOWLEDGEMENTS

This work was supported by the Ministry of Education and Science of Ukraine (the Young Scientist projects № 0120U101064 "Novel nanomaterials based on the lyophilic self-assembled systems: theoretical prediction, experimental investigation and biomedical applications" and the project № 0119U002525 "Development of novel ultrasonic and fluorescence techniques for medical micro- and macrodiagnostics").

ORCID IDs

Uliana Tarabara, https://orcid.org/0000-0002-7677-0779; **Olga Zhytniakivska,** https://orcid.org/0000-0002-2068-5823
Kateryna Vus, https://orcid.org/0000-0003-4738-4016; **Valeriya Trusova,** https://orcid.org/0000-0002-7087-071X
Galyna Gorbenko, https://orcid.org/0000-0002-0954-5053

REFERENCES

[1] R. Gallardo, N.A Ranson, S.E Radford, Curr. Opin. Struct. Biol. **60**, 7-16 (2020). https://doi.org/10.1016/j.sbi.2019.09.001.
[2] V. Martorana, S. Raccosta, D. Giacomazza, L. A. Ditta, R. Noto, P. L. S. Biagio, M. Manno, Biophys. Chem. **253**, 106231 (2019). https://doi.org/10.1016/j.bpc.2019.106231.
[3] C.M. Dobson, Cold Spring Harb. Perspect. Biol. **9**, a023648 (2017). https://doi.org/10.1101/cshperspect.a023648.
[4] P. C. Ke, R. Zhou, L. C. Serpell, R. Riek, T. P. J. Knowles, H. A. Lashuel, E. Gazit, I. W. Hamley, T. P. Davis, M. Fändrich, D. E. Otzen, M. R. Chapman, C. M. Dobson, D. S. Eisenberg, R. Mezzenga, Chem. Soc. Rev. **49**, 5473-5509 (2020). https://doi.org/10.1039/C9CS00199A.
[5] O.S. Makin, L.C. Serpell, FEBS J. **272**, 5950-5961 (2005). https://doi.org/10.1111/j.1742-4658.2005.05025.x.
[6] R. Nelson, D. Eisenberg, Curr. Opin. Struct. Biol. **16**, 260-265 (2006). https://doi.org/10.1016/j.sbi.2006.03.007.
[7] Z. Wang, S. Kang, S. Cao, M. Krecker, V. Tsukruk, S. Singamaneni, MRS Bulletin **45**, 1017-1026 (2020). https://doi.org/10.1557/mrs.2020.302.
[8] T.P.J. Knowles, R. Mezzenga, Adv. Mater. **28**, 6546-6561 (2016). https://doi.org/10.1002/adma.201505961.
[9] M. Stefani, Biochim. Biophys. Acta, **1739**, 5-25 (2004). https://doi.org/10.1016/j.bbadis.2004.08.004.

[10] F. Chiti, C. M. Dobson, Annu. Rev. Biochem., **75**, 333-366 (2006). https://doi.org/10.1146/annurev.biochem.75.101304.123901.
[11] M. Bucciantini, S. Rigacci and M. Stefani, J. Phys. Chem. Lett., **5**, 517-527 (2014). https://doi.org/10.1021/jz4024354.
[12] S. M. Butterfield and H. A. Lashuel, Angew. Chem., Int. Ed.,2010, **49**, 5628-5654. https://doi.org/10.1002/anie.200906670.
[13] A. A. Meratan, A. Ghasemi and M. Nemat-Gorgani, J. Mol.Biol., **409**, 826-838 (2011). https://doi.org/10.1016/j.jmb.2011.04.045.
[14] B. Huang, J. He, J. Ren, X. Y. Yan and C. M. Zeng, Biochemistry, **48**, 5794-5800 (2009). https://doi.org/10.1021/bi900219c.
[15] B. Caughey, P. T. Lansbury, Annu. Rev. Neurosci., **6**, 267-298 (2003). https://doi.org/10.1146/annurev.neuro.26.010302.081142.
[16] E. Sparr, M. F. M. Engel, D. V. Sakharov, M. Sprong, J. Jacobs, B. de Kruijf, J. W. M. Hoppener, J. A. Killian, FEBS Lett., **577**, 117-120 (2004). https://doi.org/10.1016/j.febslet.2004.09.075.
[17] M. F. Engel, L. Khemtemourian, C. C. Kleijer, H. J. Meeldijk,J. Jacobs, A. J. Verkleij, B. de Kruijff, J. A. Killian and J. W. Ho ¨ppener, Proc. Natl. Acad. Sci. U. S. A., **105**,6033-6038 (2008). https://doi.org/10.1073/pnas.0708354105.
[18] A. L. Gharibyan, V. Zamotin, K. Yanamandra, O. S.Moskaleva, B. A. Margulis, I. A. Kostanyan and L. A.Morozova-Roche, J. Mol. Biol., **365**, 1337-1349 (2007). https://doi.org/10.1016/j.jmb.2006.10.101.
[19] J.F. Brandts, L.J. Kaplan, Biochemistry **12**, 2011-2024 (1973). https://doi.org/10.1021/bi00734a027.
[20] M. Groenning, J. Chem. Biol. **3**, 1-18 (2010). https://doi.org/10.1007/s12154-009-0027-5.
[21] V.M. Ioffe, G.P. Gorbenko, T. Deligeorgiev, N. Gadjev, A. Vasilev, Biophys. Chem. **128**, 75–86 (2007). https://doi.org/10.1016/j.bpc.2007.03.007.
[22] M. Bacalum, B. Zorila, M. Radu, Anal. Biochem. **440**, 123–129 (2013). https://doi.org/10.1016/j.ab.2013.05.031.
[23] J.R. Lakowicz, Principles of fluorescence spectroscopy, 3rd ed., (Springer, New York, 2006).
[24] G. Gorbenko, O. Zhytniakivska, K. Vus, U. Tarabara, V. Trusova, Phys. Chem. Chem. Phys. **23**, 14746-14754 (2021), https://doi.org/10.1039/D1CP01359A.
[25] I. M. Kuznetsova, A.I. Sulatskaya, V. N. Uversky, K. K. Turoverov, Mol. Neurobiol. **45**, 488-498 (2012). https://doi.org/10.1007/s12035-012-8272-y.
[26] H. Xie, C. Guo, Front. Mol. Biosci. **7**, 629520 (2021). https://doi.org/10.3389/fmolb.2020.629520.
[27] K. Siposova, M. Kubovcikova, Z. Bednarikova, M. Koneracka, V. Zavisova, A. Antosova, P. Kopcansky, Z. Daxnerova, Z. Gazova, Nanotechology, 23, 055101 (2012). https://doi.org/10.1088/0957-4484/23/5/055101.
[28] U. Bohme, U. Scheder, Chem. Phys. Lett., **434**, 342–345 (2007). https://doi.org/10.1016/j.cplett.2006.12.068.
[29] G. Sudlow, D. J. Birkett, D.N. Wade, Mol. Pharmacol., **12**, 1052–1061 (1976).
[30] A. Samanta, S. Jana, D. Ray, N. Guchhait, Spectrochim. Acta. A, **121**, 23-34 (2014). https://doi.org/10.1016/j.saa.2013.10.049.
[31] V. S. Jisha, K. T. Arun, M. Hariharan, D. Ramaiah, J. Phys. Chem. B, **114**, 5912-5919 (2010). https://doi.org/10.1021/jp100369x.
[32] G. Gorbenko, V. Ioffe, P. Kinnunen, Biophys J., **93**, 140-153 (2007). https://doi.org/10.1529/biophysj.106.102749.
[33] G. Gorbenko, V. Ioffe, J. Molotkovsky, P. Kinnunen, Biochim. Biophys Acta, **1778**, 1213-1221 (2008). https://doi.org/10.1016/j.bbamem.2007.09.027.
[34] G. Ghosh, L. Panicker, K.C. Barick, 118, 1-6 (2014). https://doi.org/10.1016/j.colsurfb.2014.03.026.
[35] L. Li, W. Xu, H. Liang, L. He, S. Liu, Y. Li, B. Li, Y. Chen, 126, 459-466 (2015). https://doi.org/10.1016/j.colsurfb.2014.12.051.

ФЛУОРЕСЦЕНТНЕ ДОСЛІДЖЕННЯ ВЗАЄМОДІЇ МІЖ АМІЛОЇДНИМИ ФІБРИЛАМИ ІНСУЛІНУ ТА БІЛКАМИ

У. Тарабара, О. Житняківська, К. Вус, В. Трусова, Г. Горбенко

Кафедра медичної фізики та біомедичних нанотехнологій, Харківський національний університет імені В.Н. Каразіна м. Свободи 4, Харків, 61022, Україна

Самоорганізація білків та пептидів в амілоїдні фібрили є предметом інтенсивних досліджень, оскільки встановлено зв'язок цього процесу з численними захворюваннями людини. Незважаючи на значний прогрес у розумінні цитотоксичності амілоїдів, роль клітинних компонентів, зокрема білків, у цитотоксичній дії амілоїдних агрегатів досі повністю не з'ясована. Дана робота спрямована на вивчення взаємодії між амілоїдними фібрилами інсуліну та деякими білками, які відрізняються за своєю структурою та фізико-хімічними властивостями. З цією метою, було досліджено флуоресцентні спектральні властивості амілоїд-чутливого фосфонієвого барвника TDV у фібрилах інсуліну (InsF) та їх сумішах із нативним сироватковим альбуміном (SA), лізоцимом (Lz) та інсуліном (Ins), частково розгорнутими при низькому pH. Виявилось, що зв'язування TDV з амілоїдними фібрилами інсуліну супроводжується значним зростанням інтенсивності флуоресценції. У системі (InsF + TDV) спектри флуоресценції зонду можна розкласти на три спектральні компоненти з максимумами на довжинах хвиль~ 572 нм, 608 нм і 649 нм. Додавання SA, Lz або Ins до суміші (InsF + TDV) призводило до зміни інтенсивності флуоресценції, положення максимуму флуоресценції та відносного внеску першої та третьої спектральних компонентів у загальний спектр. Для отримання додаткової інформації щодо взаємодії між амілоїдними фібрилами інсуліну та білками досліджено Фьорстерівський резонансний перенос енергії між TDV у якості донора, і скваранового барвника SQ1 як акцептора. Встановлено, що SA не змінює ефективність переносу енергії порівняно з контрольною системою (InsF + хромофори), тоді як додавання Lz та Ins призвело до зниження ефективності. Зміни флуоресцентного відгуку TDV в системах білок-фібрили можна пояснити перерозподілом молекул зонду між сайтами зв'язування, розташованими на InsF, нефібрилізованих Ins, SA або Lz та інтерфейсі білок-білок.

Ключові слова: фосфонієвий зонд, амілоїдні фібрили інсуліну, комплекс фібрила-білок.